PAPER

Check for updates

Dynamic volatile insights of solid-state fermented oats with *Lactiplantibacillus plantarum*: a future food sustainable development strategy

Stella Green, [ID] [a] Graham T. Eyres,[a] Dominic Agyei,[b] Nicholas Horlacher,[a] Elisa Di Stefano[cd] and Biniam Kebede [ID] *[e]

Solid-state fermentation of oats has shown potential for bioactive enrichment and nutritional modification in the quest to develop nutritionally dense foods and meet future global food demands. However, the current body of literature on flavour aspects, such as volatile generation, is lacking. The present study aimed to monitor the volatile evolution of oats fermented using *Lactiplantibacillus plantarum* as a readily available lactic acid bacterium, followed by a regression analysis of volatile release. Ground, dehulled and stabilised oats were fermented with *Lp. plantarum* for 0, 2, 5, 12, 24, 48, 72 and 120 hours at 37 °C. Samples were subjected to headspace solid-phase microextraction gas chromatography coupled to mass spectrometry to evaluate volatile changes during fermentation. Aldehydes dominated early samples but decreased rapidly after ∼5 hours of fermentation, while furans and esters decreased to a lesser extent after 48–72 hours. Alcohols and ketones steadily increased until the end of fermentation, as did carboxylic acids and aromatic compounds, while volatile phenols were found to peak at 48 hours of fermentation. In contrast to linear partial least squares regression data modelling, non-linear random forest regression effectively accounted for the non-linear evolution of volatile formations by *Lp. plantarum*. These results shed light on the metabolic actions of *Lp. plantarum* and provide insights into the flavour potential of oats *via* solid-state fermentation while also highlighting the importance of non-linear modelling to predict volatile evolutions accurately.

Sustainability spotlight

To meet growing nutritional needs in the face of climate change, population growth, and limited resources, sustainable food innovation is critical. It is well-established that solid-state fermentation (SSF) can enrich the nutritional and bioactive profiles of oats without excess water, supporting resource-efficient processing. By monitoring volatile evolution over 120 hours of SSF, this study offers additional insights into flavour aspects and volatile markers of metabolic pathways that can be optimised for nutritionally enriched oat-based products with broader adoption in future food systems. Therefore, this work contributes to the SDGs 2 (Zero Hunger), 3 (Good Health and Well-Being), and 12 (Responsible Consumption and Production) by promoting sustainable processing of accessible, nutrient-rich crops using low-input biotechnology.

Introduction

The current food system is facing increasing pressures such as a growing population, environmental resource depletion, a changing climate, and a decline in food affordability and accessibility.[1] These pressures are projected to grow, requiring urgent innovation in food innovation to ensure future availability of nutritious, accessible, and acceptable foods.[1,2]

Oats (*Avena sativa*) are an excellent candidate to address this challenge, being a cereal that has fuelled humans for centuries thanks to their nutrient-dense nature, enabling well-developed infrastructure to grow and process them on a global scale economically. Oats generally contain more protein than most other cereals and consistently show the highest amount of unsaturated lipids.[3,4] Oats are an excellent carbohydrate source and high in dietary fibre, such as β-glucan, which is important for regulating blood sugar and supporting the growth of beneficial human gut microbiota.[4] When considering the need for the development of future food with acceptable flavour properties and elevated nutritional properties, oats could also benefit from further sustainable processing.[5] Specifically, bioactive enrichment, nutritional modification to further bolster protein, and flavour modifications could position oats to

[a]*Department of Food Science, University of Otago, Dunedin 9016, New Zealand*

[b]*School of Chemistry, Monash University, Melbourne, Victoria 3800, Australia*

[c]*APC Microbiome Ireland, University College Cork, Western Road, Cork, Ireland*

[d]*School of Microbiology, University College Cork, Cork, Ireland*

[e]*Department of Food Science, University of Guelph, Guelph, Ontario N1G 2W1, Canada. E-mail: biniam@uoguelph.ca; Tel: +1 (519) 993 1711*

better meet dietary needs with broader uptake into future food systems.

Solid-state fermentation (SSF) presents an opportunity to naturally and economically process oats into new sensory and nutritional potentials for future food development. Fermentation is a naturally sustainable mode of capitalising on microorganisms' metabolisms to modify the initial substrate's composition, microstructure, and flavour components into new novel characteristics. SSF forgoes the addition of free-flowing water, making it more resource-efficient than its submerged (SmF) counterpart.[6]

It has been established that processing oats *via* SSF can yield improved bioactive contents and activities, and in some cases, improve the protein content.[5,7,8] However, to date, few studies have considered flavour aspects of SSF cereal-based products, let alone oats, a necessary aspect to consider in the development of future food.[9–11] Unprocessed oats could benefit from processing such as SSF to decrease "grassy" flavoured volatile aldehydes that are naturally present and enrich novel, pleasant flavours. Volatile compounds can not only contribute new novel flavours, but they can also provide insights into metabolic pathways of the microorganisms involved.[12] Gaining a better understanding of what metabolic pathways are favoured by sampling at various timepoints throughout SSF could aid in optimising SSF for specific volatile and nutritional outcomes, and to the best of our knowledge, has not been conducted on oats with SSF.

Lactiplantibacillus plantarum is a well-known lactic acid bacteria (LAB) used in the production of many SmF dairy-based fermented products and has exhibited flavour-active volatile production.[9,13,14] While *Lp. plantarum* is more traditionally used in SmF systems, more studies are now applying this species to SSF systems for flavour, fermentation trackability, potential probiotic, and consumer familiarity advantages.[9,14–16] Previous work has demonstrated the ability of *Lp. plantarum* strains to improve B vitamin content, probiotic properties, bioactive properties, and functional properties in plant-based substrates, including oats.[13,15,17,18]

So far, most published studies have considered volatile production and, in some cases, evolution of fermented oats in SmF systems as opposed to SSF systems.[14,19–21] While[9] and[10] have considered volatile productions by *Lp. plantarum* in SSF of oats, only the terminal volatiles were investigated, and no clues as to the evolution of volatiles over time were given. Monitoring the temporal evolution of volatiles is important for yielding insights into metabolic actions of the LAB and providing indications on optimal SSF length for specific volatile markers of compound classes like bioactive phenols. Moreover, neither of these studies investigated *Lp. plantarum* in a mono-culture, thus, volatiles produced were only attributable to their co-culture systems with *Saccharomyces cerevisiae* and *Rhizopus microsporus*.[9,10] Studying *Lp. planatrum* in isolation could yield further insights as to non-fungal related compounds through comparison with these findings.

This paper aimed to address the outlined research gaps by monitoring the evolution of volatiles over time during the SSF of oats over an extended time of 120 h. Through monitoring

volatile changes, insights as to the flavour-producing and metabolic actions of *Lp. plantarum* in oats can be gained in the context of the sustainable development of future food products.

Methods and materials

Solid state fermentation

Inoculum preparation. *Lp. plantarum* 299v was isolated from probiotic commercial sources and stored in glycerol stocks at −80 °C.[23] Before fermentation, cells were propagated twice in De Man, Rogosa and Sharpe broth (MRS) (Fort Richards Laboratories, Auckland, NZ) at 37 °C, overnight, anaerobically. Cells were harvested by centrifugation at $3000 \times g$ for 10 min (5810R, Eppendorf, Hamburg, Germany), washed twice in phosphate-buffered saline (PBS) and reconstituted in PBS. This was used as the inoculum for SSF.

Fermentation. Dehulled, stabilised oat groats (Harraway and Son Ltd, Dunedin, New Zealand) were cleaned and soaked in filtered water overnight at a ratio of 5 : 8 (w/w), before draining and autoclaving at 121 °C for 15 min in a 3 L glass beaker covered with tinfoil. After cooling, these were aseptically transferred to a blender and ground for 30 s in batches. The ground oatmeal was transferred to a sterile 3 L glass beaker for inoculation. Enough water sterilised by autoclaving was mixed with the prepared inoculum to ensure even dispersion. This inoculated water was combined with the oat substrate and mixed for 30 s, to ensure even distribution. A ratio of substrate to inoculated water at 5 : 6 (w/w) was used, and the inoculation rate was 1×10^6 colony-forming units (CFU) per gram of ground oatmeal. Triplicate aliquots of 70 ± 5 g of inoculated oats were weighed into sterile Petri dishes (90 mm × 20 mm, diameter × height) for each timepoint and incubated anaerobically at 37 °C for up to 120 h.

Timepoint sampling. Samples were taken at 0, 2, 5, 12, 24, 48, 72, and 120 h based on preliminary studies to capture the greatest extent of change. At each timepoint, three Petri dishes were removed and placed on ice to halt fermentation. Sampling from one Petri dish at a time, 2 × 5 g samples were taken from each dish, placed in 20 mL sample vials and stored at −60 °C for later volatile analysis. A further 5 g was placed in a beaker with 1 mL of water to sufficiently liquify the slurry and measure the pH. Finally, a 2 g sample was weighed into a Stomacher bag and diluted with 20 mL PBS, before homogenising using a paddle blender and performing a serial dilution for plating with the drop plate method to obtain the colony forming unit per gram (CFU g^{-1}) counts.

Analysis of fermented oat samples

Volatile compounds. Volatile analysis of the ferments was performed using headspace solid-phase microextraction gas chromatography coupled to mass spectrometry (HS-SPME-GC-MS) based on a previously developed method and optimised in preliminary trials.[24] HS-SPME was selected for its solvent-free, rapid, non-destructive, automated, and reproducible extraction.[25] This preserves the native aroma profile better than solvent-assisted flavour evaporation or simultaneous

distillation extraction, both of which risk loss or alteration of volatiles.[25] HS-SPME is also highly compatible with untargeted GC-MS, offering broad sensitivity across volatile classes, due to the fibre containing 3 polymers of mixed polarity, and is widely used in food volatilomics, enabling meaningful comparison with previous studies.[9,21] While HS-SPME has drawbacks such as limited capacity and underrepresentation of less volatile compounds, these were deemed acceptable given the study's focus on dominant volatiles affected by SSF over time. An Agilent Technologies 6890 N gas chromatograph (Agilent Technologies, Santa Clara, CA, USA) equipped with an autosampler (Agilent PAL RSI 85; Palo Alto, CA, USA) was used for analysis. Samples were thawed and kept in a cooled tray at 4 °C before analysis, as determined in preliminary trials to adequately halt further fermentation of the samples. Sample order was randomised to minimise potential order effects, and blanks were run before and after daily runs to monitor for carryover. For headspace volatile extraction, vials were incubated at 40 °C for 5 min with agitation to reach an equilibrium state. A divinylbenzene/carboxen/polydimethylsiloxane mixed-polarity SPME fibre (50/30 μm) (Supelco Inc, Bellefonte, PA, USA) was exposed to the headspace of the vial for 30 min at 40 °C to extract the volatiles.

Desorption of analytes into the GC-MS oven was carried out in splitless mode for 2 min, with a constant flow rate of 1 mL min^{-1} using helium as the carrier gas. A 59 m polar Zebron ZB-WAX column (Phenomenex, Torrance, CA, USA) was used for analyte separation. The GC oven program began at 50 °C held for 5 min, followed by an increase to 210 °C at a rate of 5 °C min^{-1}. The temperature then increased again to 240 °C at a rate of 10 °C min^{-1}, with a final hold time of 20 min at this temperature. Mass spectra were measured with an Agilent 5975B VL MSD (Agilent Technologies, Santa Clara, CA, USA) containing a triple-axis detector in electron ionisation mode with an energy of 70 eV in the range of 29–300 m/z.

Alkane standards from C_7–C_{30} were injected with the same method to calculate the linear retention indices (RIs). Volatiles were tentatively identified using three, preestablished criteria: (1) by comparing the deconvoluted mass spectra to the National Institute of Standards and Technology 2014 (NIST14) spectral library with a minimum fit quality threshold of 80%; (2) comparison of the calculated RIs to the compound's RI reported in literature for the same column; (3) routinely matching retention time and mass spectral profiles for at least one injected reference standard of each chemical class.[26]

Data analysis

Preprocessing the volatile data. The HS-SPME-GC-MS data was exported as a Common Data Format (CDF) file into PARA-DISe (PARAFAC2 based Deconvolution and Identification System), version 3.2 (ref. 27) to deconvolute and identify the peaks.[28] Peak intervals were manually selected based on careful comparison with the overlayed replicate chromatograms and cross-checking of the blanks to retain the relevant intervals. Models were calculated for these intervals with 1–10 components and the optimal number of components for each interval was manually selected based on the following criteria: (1)

percentage fit and core consistency of the model, (2) model residuals, (3) interval mass spectrum comparison to the NIST14 library for match and probability values, (4) separate elution profiles of the components, (5) knowledge of the samples and expected volatiles for the samples. These relative concentrations based on peak area were exported for further analysis. Peak areas were used to assess relative volatile abundance without the use of internal standards, as the aim of this untargeted analysis was to monitor relative changes in dominant volatiles over time, rather than to obtain absolute concentrations.

Modelling the volatile data. Data modelling was conducted sequentially to explore the data unsupervised, before moving on to classical chemometric modelling and advanced machine learning. Preprocessing using mean centering and autoscaling was applied to the data before all modelling methods were employed. An unsupervised principal component analysis (PCA) was initially performed to explore the data trends and remove outliers for the following analyses. A supervised, linear partial least squares regression (PLS-R) was then performed. Variable importance on projection (VIP) selection of compounds was performed with VIP scores greater than 1 deemed as important features for the model's predictive ability. K-Fold cross-validation using 15 folds was used, and the number of latent variables (LVs) was determined based on minimising the root mean squared error (RMSE) while capturing the most cumulative variance. A non-linear random forest regression (RF-R) was performed on the same pre-processed data, using 10-fold k-fold cross-validation. The tuneRF function was used to optimise the maximum depth of trees (max_depth), number of trees (n_{tree}), and m_{try} to mitigate model overfitting. In-built feature selection identified features that reduced Gini impurity, a measure of uncertainty, and improved predictive importance. A threshold for Gini-importance was determined by sequentially removing features from the model from lowest Gini-importance to highest, until the model performance reduced the model performance metrics of RMSE and R^2. Based on this method, the threshold was selected as 300.

Statistical analysis

To determine significant differences between sample groups, analysis of variance (ANOVA) followed by Tukey's honestly significant difference (HSD) multiple comparison tests was used.

All data analyses and modelling were performed using the statistical software R version 4.4.2 (Ref. 29) and the RStudio[30] integrated development environment to model the data, generate score plots, multidimensional scaling (MDS) plots, heatmaps, and box plots as part of this process, and to perform ANOVA and Tukey HSD.

Results and discussion

Characterising the SSF

Changes in viable cell counts and pH during 120 h of oat SSF with *Lp. plantarum* can be found in Fig. 1. A rapid increase in bacterial population is observed between 2 and 12 h of
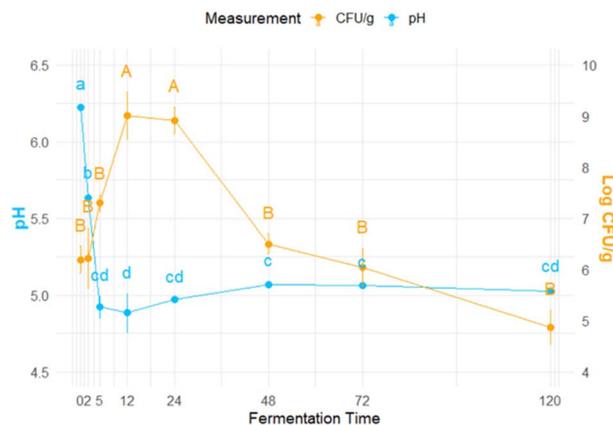
Fig. 1 Changes in *Lp. plantarum* viable cell counts (orange, with capital letters indicating significant differences to $p < 0.05$) and pH (blue with lower case letters indicating significant differences to $p < 0.05$).

fermentation, changing from 6.21 log CFU g^{-1} to 9.01 log CFU g^{-1} with statistical significance ($p < 0.05$). This remained stable until 24 h before dropping back to the 0 h range of viable cells, with a significant difference ($p < 0.05$) by 48 h. Beyond 48 h, there were no further statistically significant changes to the CFU per g counts. This neatly demonstrates a traditional bacterial growth curve of a slight lag phase between 0–2 h, a logarithmic phase between 2 and 12 h, a stationary phase between 12 and 24 h before beginning to enter the decline phase at some point after 24 h onwards.[31] Although there is no statistically significant difference in CFU g^{-1} from 48 h onwards, the decreasing slope suggests that with further time point sampling, beyond 120 h of SSF, a significant difference would be found. In terms of the LAB system, this indicates that the cells fermented the oat substrate successfully in the solid-state conditions. It also shows that cells were still viable by 120 h of SSF, suggesting that volatile profiles may still be changing due to the available enzymatic power of the live cells, although likely at a reduced rate compared with the high number reported between 12–24 h. Most other papers halt fermentation by 48–72 h, when viable cell counts are still high or just starting to drop, but this does not explore the full volatile potential.[7,9,32] By fermenting for an extended period, stabilised volatile peak areas, additional volatile concentration changes, or increased volatile diversity may be observed.

A complementary mode of monitoring LAB fermentation was to measure changes in pH. Fig. 1 shows a rapid drop in pH from 0 to 5 h, from 6.22 to 4.92, before reaching the minimum at 12 h (4.88), then buffering slightly to oscillate around 5.00 until reaching a terminal pH of 5.02. Buffering could be ascribed to the ammonia production by the LAB as an acid stress response to regulate intracellular pH.[33] Unlike viable cell count, pH drop infers metabolic insights as it reflects the accumulation of lactic acid and other organic acids produced by the LAB during fermentation. This also explains why the drop in pH occurs slightly before the maximum viable cell count, as this shows that during the logarithmic stage of growth, the cells were

metabolising the oat substrate most rapidly to sustain population growth, thus producing more acids to reduce pH. The pH drop demonstrated here is again in line with expected trends for *Lp. planatrum*.[34] Once again, this pH drop implies successful fermentation of the oat substrate using *Lp. planatrum* and the potential for a range of volatile products.

Volatile changes

Evolution of chromatogram peaks over SSF time. Clear differences between all sampled timepoints of SSF were observed with minimal background, validating the volatile analysis method used. Fig. 2A overlays the 0, 48 and 120 h time moment chromatograms for the retention time relevant to key compounds later identified through peak deconvolution. Even at this level, a clear trend of mostly early eluting compounds decreasing from time 0 onwards and most other peaks increasing with time can be observed. A few compounds can be seen to peak after 48 h of fermentation, signifying oats fermented to middle timepoints may be distinctively different in their volatile profiles to more extended fermentation times. In terms of background, this chromatogram shows a relatively consistent baseline, indicating minimal noise and carryover between HS-SPME-GC-MS runs. This signifies good sensitivity and reliable peak identification.[35] This exemplifies the successful performance of volatile separation using the present method and validates further analysis on key differences between different fermentation times with *Lp. plantarum*.

Key changes in volatile classes over SSF time. After validating the HS-SPME-GC-MS method, the peaks were deconvoluted, identified and classified into different chemical classes for each time moment. In total, 55 compounds were detected, spanning 10 chemical classes: 2 acetals, 8 alcohols, 4 aldehydes, 5 aromatic compounds, 7 carboxylic acids, 14 esters, 3 furans, 8 ketones, 3 phenols and 1 terpenoid (Table S1).

Based on the sum of peak areas for relative concentrations of volatiles, the proportion of volatile compound classes changed significantly throughout SSF (Fig. 2B). Fig. 2C sheds further light on the individual magnitudes of peak area changes for each chemical class. Fig. 2B highlights that most of the proportionality change in chemical classes overall occurs within 24 h of SSF, after which the relative proportions of chemical classes fluctuate around similar levels. This reflects the fermentative nature of *Lp. planatrum*, where the most drastic changes in fermentation are often shown to occur rapidly within the first 6–8 h of fermentation, in line with the logarithmic phase of growth and the drop in pH, before the viable cell population stabilises, as exemplified in Fig. 1.[34]

At 0 h of fermentation, when *Lp. plantarum* is added to the oats, the greatest proportion of volatiles was aldehydes (35.74%), followed by esters (26.05%) (Fig. 2B). By the end point of fermentation, the inverse is true, and alcohols and ketones dominate the fermented products, with 37.11% and 36.47% respectively. This is in line with other studies, reflecting the composition of unfermented oats containing high levels of unsaturated fatty acids such as linoleic acid and oleic acid, which are oxidised over time *via* lipase to yield an accumulation of aldehydes.[9,14] At the starting
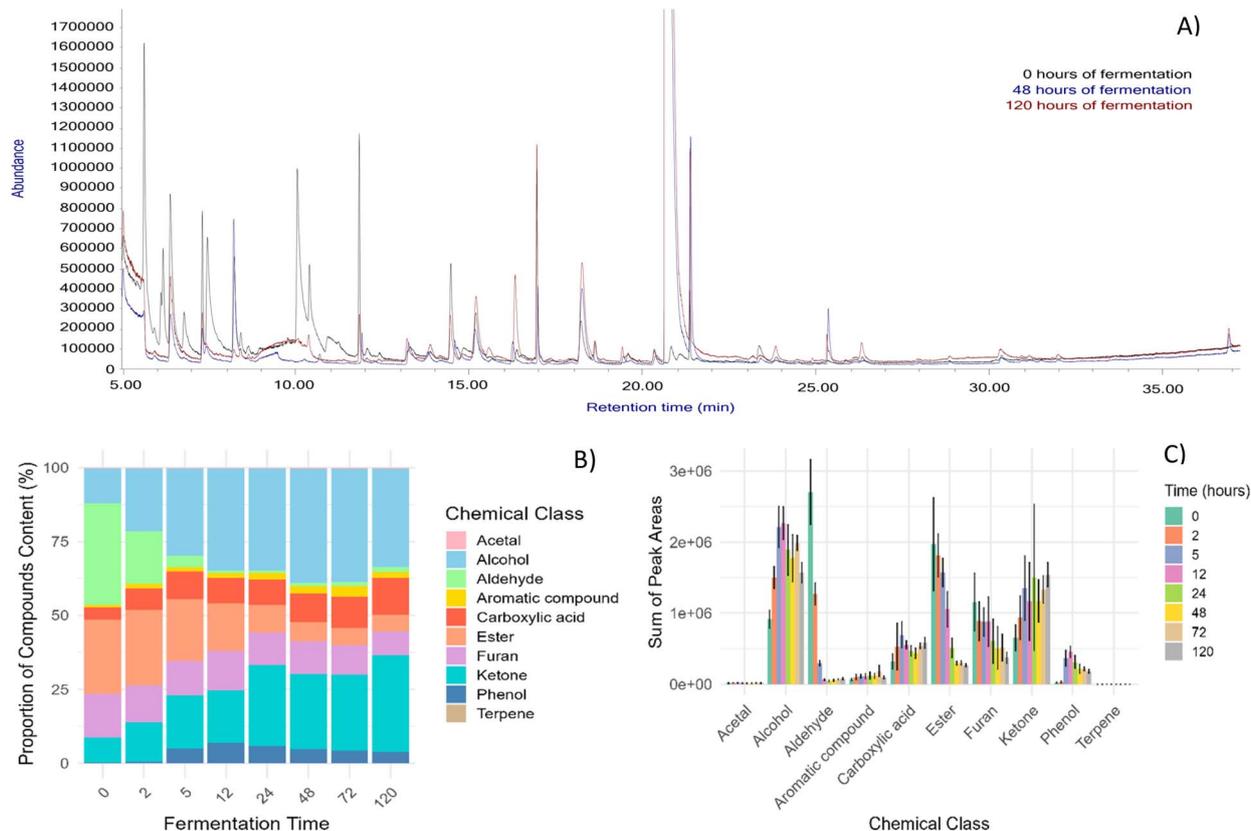
Fig. 2 Changes in oat volatiles over the course of 120 h of solid-state fermentation. (A) Overlayed chromatogram of 0 (black), 48 (blue), and 120 (red) h of SSFed oats. (B) Summed proportions of peak areas for each chemical class at each sampled timepoint. (C) Dynamic changes in chemical class peak areas at each sampled timepoint. Error bars denote standard deviations.

point of SSF, these are shown to be at their highest summed amount (Fig. 2C), but SSF with *Lp. planatrum* significantly reduced these to a negligible amount within 5–12 h. In terms of flavour profiles, this can be advantageous as aldehydes can impart green, rancid notes onto the oat product.[19,36]

Aldehydes are susceptible to reduction reactions due to the slightly positive charge on their carbon atom, making them highly attractive to nucleophiles.[37] This makes them susceptible to reduction reactions to yield alcohols and oxidation reactions to yield acids, which can react further to form esters.[37,38] *Lp. plantarum* contains aldehyde dehydrogenases that can catalyse these reactions.[21] In this mode, increasing the length of SSF time decreased aldehydes overall by 12.7% and increased alcohols by 71.3% and acids by 80.7% as downstream products, by 120 h. This proportionality effect was indeed observed in Fig. 2B and C. This trend agrees with previous literature reporting on fermentation to yield acids and alcohols to varying lengths of SSF.[11,22,39–42]

Ketones also began to dominate the proportion of total compound peak area towards the later SSF times, as shown in Fig. 2B.[36] Looking solely at the change in ketones during fermentation in Fig. 2C, these increase rapidly from 0–5 h of SSF before fluctuating around the same level until 120 h with an overall 135.8% increase. This can be explained by the autooxidation of the naturally occurring unsaturated fatty acids found in raw oat substrate *via* β-oxidation.[4,37] Specifically, *Lp.*

planatrum as a LAB can anaerobically metabolise citrate and pyruvate, yielding acetoin and diacetyl ketones, which are known for their buttery characters.[21] These can also be produced *via* upstream lipolytic pathways, generating fatty acid precursors as well as amino acid catabolism.[9] Similar trends of enhanced volatile ketone content were observed by[19] for *Lp. plantarum* fermented oats, albeit in a submerged system. This validates the present findings and demonstrates the application of *Lp. plantarum*'s to enrich ketones in both SSF and SmF fermentation systems. The initial presence of ketones is as expected due to the intrinsic oat lipase oxidising the high levels of unsaturated fatty acids as the oats are stored.

Furans are also generated as downstream products of aldehydes, again reflected in their highest levels at the start of fermentation (Fig. 2C and B). Moreover, pre-treating the oats with heat to stabilise and inactivate their enzymes likely generates a portion of these furans *via* the thermal degradation of the carbohydrates, protein, and lipids which were quantified in the initial oat substrate in the supplementary information (Table S2).[43] While other oat fermentation studies on volatile compounds report some level of furans by the end of fermentation, the change in their content overall is not often significantly different from the starting material.[9,21] The reduction in furans shown here may be attributed to SSF times of longer than 48 h and may be important for reducing bitter, burnt and roasty flavours.

Phenols and aromatic compounds provide insight as to the potential bioactive enrichment. of the oat samples. Specifically, phenols can impart antioxidant properties to the final oat product.[5] Their volatile enrichment can signify their overall improved liberation from the oat substrate, where they are normally tightly bound. Fig. 2C shows that volatile phenols increased drastically after only 5 h of SSF, peaking at 12 h with a 2007.9% increase in peak area, before decreasing somewhat by 120 h, yielding a terminal 738.9% increase relative to 0 h. Total aromatic compounds also increased by 53.6% after 120 h of SSF (Fig. 2C). For future work, this may imply that 12–48 h of SSF may favour the greatest phenolic enrichment.[9] similarly reported an overall increase in phenolic compounds by the end of SSF with *Lp. plantarum* in co-inoculation with *S. cerevisiae*. Therefore, the present study highlights the ability of *Lp. plantarum* to enrich this class of compounds without the need for additional microorganisms to mobilise certain precursor products first, as suggested by ref. 9.

Esters steadily decreased over the course of SSF from 0 to 48 h, as depicted in their proportionality in Fig. 2B and their overall decrease in Fig. 2C. This is not in line with currently published literature, where most report their increase due to esterase condensation of alcohols and acids.[9] This may be due to the lack of a co-culture used in the present study and may reflect the preference of *Lp. plantarum*'s metabolism towards other pathways.

Modelling of volatile data

Linear PLS-R performance. After characterising the evolution of general chemical class changes over SSF, a traditional PLS-R chemometric model and a more advanced machine learning RF-R model were applied to the volatile data to investigate changes in specific compounds over time. Before performing these analyses, an unsupervised PCA analysis was performed to explore the data trends, which resulted in the removal of one outlier sample (Fig. S1). PCA also showed clear trends in separating different timepoints, validating further modelling with the aforementioned methods. Fig. 3 summarises the model results for PLS-R and RF-R in their respective visualisation plots, heatmaps of their feature-selected compounds, and their combined model metrics.

In terms of the initially performed linear PLS-R, three LVs were selected as optimal based on maximising explained variance and minimising RMSE of prediction, explaining 54.51% cumulative variance. Fig. 3a demonstrates separation between timepoints sequentially along LV1, with every second timepoint being almost completely separated from the timepoints two either side. The similar magnitudes of grouped samples' separation indicate that the changes to the volatile profile are closer to linear, and the magnitude of profile evolution from one timepoint to the next is similar. This validates good timepoint sampling to capture the change between time moments, but further modelling and analysis is needed to confirm this. There
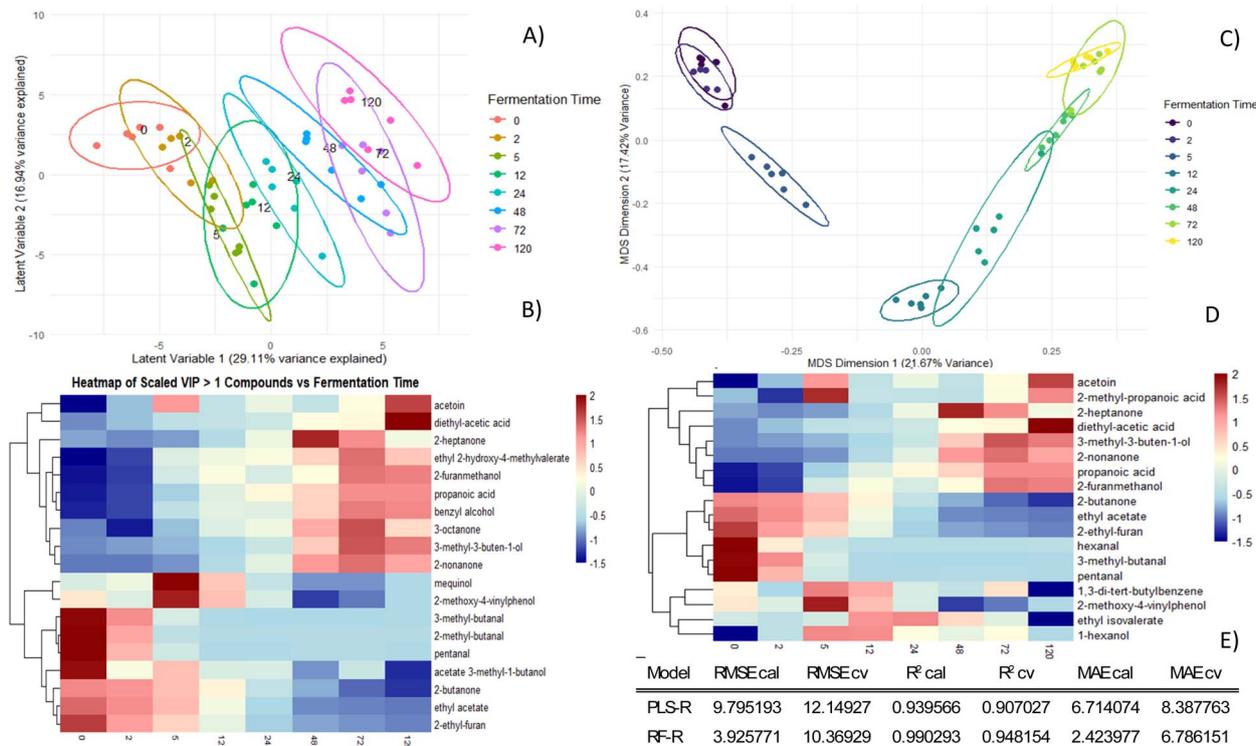

Model	RMSE cal	RMSE cv	R² cal	R² cv	MAE cal	MAE cv
PLS-R	9.795193	12.14927	0.939566	0.907027	6.714074	8.387763
RF-R	3.925771	10.36929	0.990293	0.948154	2.423977	6.786151

Fig. 3 Modelling of HS-SPME-GC-MS volatile data over fermentation time. (A) Loadings plot visualisation of PLS-R model with 95% confidence interval ellipses. (B) Heatmap of feature-selected compounds (VID >1) for PLS-R. (C) MDS plot visualisation of RF-R model with 95% confidence interval ellipses. (D) Heatmap of the feature-selected compounds (mean decrease in Gini impurity >600) for RF-R. (E) Model performance metrics for calibration (cal) and cross-validation (cv) for both models.

does appear to be a slight separation between middle time-points and earlier and later timepoints on the second LV, indicating that some non-linearity may be present in the data. This may make PLS-R less than optimal for the data, as this is a linear model and will feature select compounds in a linear fashion.[44] Compounds that peaked in the middle of SSF may contribute to this non-linearity in the data, such as phenols (Fig. 2C), and risk not being selected as important features by this model despite being important in characterising SSF over time.

VIP analysis of the PLS-R modelled data selected a total of 19 compounds to be important in driving the separation of samples based on fermentation time, as highlighted in the heatmap (Fig. 3B). Seventeen of these compounds were either highest near the beginning or end of fermentation, and only two compounds that peaked at the mid-points of fermentation were selected: mequinol and 2-methoxy-4-vinylphenol, also known as 4-vinylguaiacol.

In terms of model metrics, PLS-R only managed to obtain RMSE values of 9.7952 and 12.1493 for calibration (cal) and cross-validation (cv), respectively (Fig. 3E). RMSE quantifies the average magnitude of errors between predicted and actual values, providing a measure of prediction performance, with lower values being better. Considering the large scale of the peak area volatile data modelled, these values are okay but could be improved. R^2 values measure how well the proportion of variance of time is explained by the volatile data using this model, explaining the goodness of fit with values closer to 1 indicating better performance. PLS-R obtained R^2 values of 0.9396 and 0.9070 for cal and cv, respectively. While values over 0.9 are considered good, alternative modelling may improve these values further.[9,44]

Non-linear RF-R performance. Considering that RF-R is a non-linear modelling method, this model was applied to the same volatile data following PLS-R in the hopes of improving model metrics and feature selection further. The tuning parameter mtry, dictating how many features are randomly sampled at each decision tree to prevent overfitting, was held constant at 27, and ntree was set to 500. These parameters were optimised using the out-of-bag error rates, applying samples not selected *via* bootstrapping in training the model, to the model and quantifying their error rates as a mode of internal cross-validation.[44] The MDS plot shown in Fig. 3C visualises RF-R with some limitations. MDS plots are constructed by reducing the dimensionality of the data to plot the samples in a lower dimensionality space, visualising relationships between samples in a similar interpretation to the loadings plot generated for PLS-R.[45] The main limitation here is that the plot is based on the proximity matrix of the RF-R model only and therefore, may not represent the true data structure. However, compared with other non-linear machine learning models like XG-BOOST, having some visualisation is better than none for interpretability of results.[45]

The MDS plot (Fig. 3C) shows better separation of samples over time for solid state fermentation along the *x*-axis with less overlap than the PLS-R model. It does appear that the last two samples at 72 h and 120 h had little difference between them in

their volatile profiles, shown by their severe overlap in the MDS plot, and to a lesser extent in the PLS-R loadings plot. This may be important in optimising extended SSF for greater bioactive liberation or other parameters, as the volatile profile appears to stay stable between 72 h and 120 h of SSF with *Lp. plantarum*. In contrast to PLS-R, the RF-R MDS plot also shows significant separation along the *y*-axis, particularly for samples in the middle timepoints 5, 12, 24 and 48 h. This may indicate better modelling of the volatiles peaking or troughing in the mid-points of fermentation as opposed to PLS-R as a linear method. However, the significant overlap of the 0 and 2 h samples shown in this MDS plot does not reflect the rapid changes observed for pH drop shown in Fig. 1. PLS-R did show more differences between these early fermentation samples, but still not a significant amount. This may simply reflect that while rapid changes are happening LAB metabolism, there is a delay in the accumulation and degradation of volatiles as the metabolism rate increases and more precursors need to be produced first. While no other papers have yet tracked volatile production over time in the SSF of oats with *Lp. planatrum*, this trend is in line with other LAB, such as *Streptococcus thermophilus* in the SmF of milk, showing a similar trend.[46]

Mean decrease in Gini-impurity is RF-R's built-in feature selection function that works by measuring how much the Gini impurity decreases each time a feature (volatile) is added to a decision split and is weighted by how many samples were affected. Compounds selected by RF-R are presented in Fig. 3D as a heatmap across the sampled timepoints of SSF. A total of 18 compounds were selected by this method, similar to PLS-R's feature selection. The feature-selected compounds largely peak at SSF timepoint 0 h or 120 h; however, RF-R was far superior to PLS-R in selecting compounds that peaked at between 12–48 h, such as 2-methoxy-4-vinylphenol, 2-heptanone, 1,3-di-*tert*-butylbenzene, ethyl isovalerate and 1-hexanol. This shows a much better selection of non-linear compounds that are likely important for SSF samples after 5–48 h and may be what aids in differentiating these samples better in the MDS plot (Fig. 3C).

In terms of model metrics, RF-R largely performed better than PLS-R as well. RMSE for calibration and cross-validation were improved to 3.9258 and 10.3693, respectively, and R^2 values for calibration and cross-validation were improved to 0.9903 and 0.9482, respectively (Fig. 3E). This further validates RF-R's ability to model the data and overall shows that this machine learning model can deal with the non-linearity in the volatile changes for oats fermented with *Lp. planatrum via* SSF. Future studies should consider using non-linear machine learning models to fit their data for differing points to obtain better outcomes in prediction, especially with more complex SSF systems, including co-culture systems.[47]

Trends in feature-selected volatiles

Feature selection informs which volatile compounds (features) have the greatest effect on improving a model's predictive performance for predicting SSF duration in this context. Trends on selected volatile compounds over SSF time are highlighted in Fig. 4 and grouped based on their feature selection by the two

models used. Overall, both models', PLS-R and RF-R feature selection functions, VIP and Gini importance, were able to select 13 of the same compounds from a broad range of chemical classes (Fig. 4), including furans, aldehydes, ketones, carboxylic acids, alcohols, esters, and volatile phenols. A few representative compounds highlighting this can be observed in
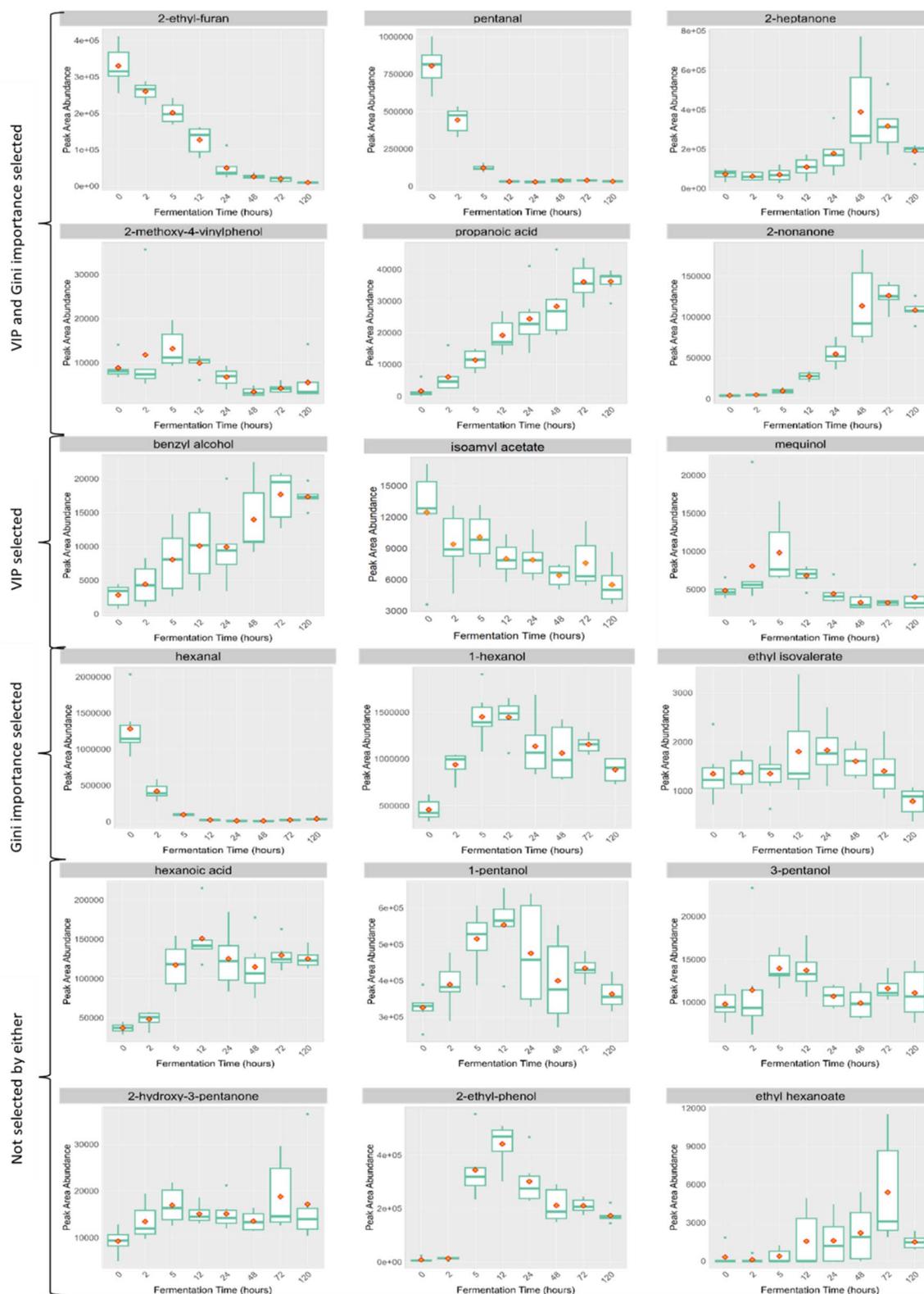

Fig. 4 Peak area boxplots of selected volatile compounds sorted based on which model's associated feature selection function was able to select them.

© 2025 The Author(s). Published by the Royal Society of Chemistry

the top two rows of Fig. 4. This demonstrates both models' weighting of a variety of chemical compound classes in their construction.

Trends in compounds feature-selected for both models include fewer volatiles that contained outlier samples falling outside of the box trends over SSF time (Fig. 4). Secondly, only relatively linear increasing or decreasing compounds were selected (Fig. 4). 2-Methoxy-4-vinylphenol was the exception to this, peaking at around 5 h of SSF before decreasing to a negligible peak area. It is important to capture compounds that also peak in the midpoints of fermentation, as these may be important for characterising these midpoints and will likely be intermediate compounds that can be metabolised further to yield the terminal and feature-selected compounds, offering valuable metabolic insights.

VIP selected compounds not selected as important by RF-R's Gini importance scores mainly included additional compounds that also either steadily increased or decreased over 120 h of SSF with *Lp. plantarum*. This can be seen in Fig. 4, row 3, except for the phenol mequinol. This differs from the additional five compounds feature-selected by RF-R's inbuilt Gini importance, which selected more compounds that peaked during the midpoints of SSF (Fig. 4, row 4). Secondly, Gini importance was able to select both hexanal and 1-hexanol, volatiles that are metabolically linked to each other, as discussed in the following metabolic insights section. The fact that RF-R regarded more compounds that peaked in the middle of SSF as important in the construction of the model may have resulted in the lower RMSE and higher R^2 values observed in Fig. 3E for RF-R. This speaks to the non-linear nature of the model and again can explain why less linearly evolving volatiles may have been selected for in this model. This further supports the notion that non-linear modelling methods should be used in future to model the progress of SSF with LAB organisms like *Lp. plantarum*.

In terms of the 31 volatiles that were not selected by either model, upon closer inspection of individual volatile boxplots, roughly half showed no obvious trend in peak area over time. The other half indicated some change, although most contained sample outliers at certain timepoints. A few examples of these are highlighted in Fig. 4, rows 5 and 6. Interestingly, there were still some compounds that appeared to significantly change to peak in the middle timepoints that were not at all feature-selected, such as 2-ethyl-phenol. This may reflect a combination of modelling and data-related limitations. Specifically, collinearity, where two volatiles show strong pairwise correlation, and multicollinearity, where several volatiles co-vary due to shared metabolic origins during SSF, are important factors.[48] PLS-R handles multicollinearity through dimensionality reduction but tends to prioritise features that explain the greatest variance in its LVs, potentially overlooking biologically relevant yet redundant volatiles.[48] Although RF-R is a non-linear model and more tolerant of correlated inputs, its use of node-splitting logic means that highly correlated volatiles can compete during model construction, resulting in one multicollinear variable dominating while suppressing others.[44,48] This effect appears to be less severe in RF-R

compared to the dimensionality reduction in PLS-R, as shown by the higher number of mid-peaking volatiles selected by RF-R and improved performance metrics. However, further work testing models for better management of multicollinearity, such as non-linear support vector machines and XGBoost may further improve feature selection for better model construction.[44]

Generally, the non-feature-selected compounds were less clear in their overall trends over time, with greater biological variation, or lower peak intensities which may fall below the signal threshold needed to contribute meaningfully to either model's performance.[49] Nevertheless, the successful classification of fermentation timepoints, the selection of compounds from a diverse range of chemical classes, and the inclusion more mid-SSF peaking volatiles than PLS-R all demonstrate that RF-R provided robust and biologically relevant outputs in this context. Its superior performance in RMSE and R^2 metrics further supports its utility as a modelling tool for time evolving SSF volatile data.

Metabolic insights based on volatile changes

In terms of the fermentative ability of *Lp. plantarum* for oats, specific metabolic actions can be inferred upon by the range of volatile compounds recorded in the present study.

As discussed earlier regarding general chemical class changes during SSF, *Lp. plantarum* drastically decreased aldehydes during the first ~12 h of SSF of oats. Pentanal, known for its grassy and bitter aroma qualities, and hexanal, grassy and apple-like, both exhibit this trend, reducing to negligible levels in their peak areas by 12 h of SSF (Fig. 4).[50] Hexanal and pentanal are oxidation products of linoleic acid, which is abundant in unfermented oats, so their anabolism can be considered as lipid degradation products catalysed by intrinsic oat lipoxygenase.[20] Reported that two *Lp. plantarum* strains separately increased hexanal 21-fold in the first 4–12 h, before decreasing again by the terminal 24 h of SmF. This opposes the 33-fold drop with *S. cerevisiae* and *Lp. plantarum* SSF reported by,[9] which is consistent with the present study (33-fold drop). The present study with *Lp. plantarum*, exemplifies its ability to substantially reduce aldehydes successfully in mono-culture conditions after 12 h. *Lp. plantarum* does contain lipases which can further oxidise oat fatty acids into aldehydes, which may explain's[20] results. This may be favoured for in SmF systems, but not in SSF systems as shown by the present and's[9] results. Additional enzymes responsible for the reduction of these compounds include alcohol dehydrogenase yielding alcohols, aldehyde dehydrogenases yielding the carboxylic acids and acetaldehyde dehydrogenase oxidation yielding carboxylic acids *via* the citric acid cycle.[51,52] Ultimately, the present study highlighted the dominant aldehyde degrading enzymatic activity of *Lp. plantarum*. Plenty of alcohols were shown to peak in the midpoints of SSF with *Lp. plantarum* such as 3-pentanol (herbal, strong aroma), 1-pentanol (balsamic, fruity aroma), and 1-hexanol (banana-like aroma).[53,54] The increase in these compounds peaking between 5–12 h of SSF corresponds directly to the aldehydes, which are reduced by *Lp. plantarum*'s enzymes

through the addition of hydrogen atoms to aldehyde's carbonyl groups, reflecting further lipid metabolism by alcohol dehydrogenase oxidation. The oats used in the present study contained 1.5% w/w lipids (Table S2). Alcohols can also be generated by the anabolism of glucose and protein (15.7% in unfermented substrate, SI) feeding into the citric acid cycle (Table S2).[37] A similar trend was seen by[21] during SmF of oats by *Lp. plantarum*. In a SSF context,[9] found that the addition of *Lp. plantarum* to a *S. cerevisiae* inoculum, decreased the amount of 1-pentanol and 1-hexanol at 72 h compared with *S. cerevisiae* in mono-culture. Our finding of 1-pentanol increasing over time initially, before gradually decreasing after 24 h (Fig. 4), highlights the ability of *Lp. plantarum* to generate this alcohol alone. This suggests that the co-culture explored by[9] simply saw the faster evolution of this compound to acids and esters, resulting in the decrease, although the lack of a 0 h time moment in[9] impedes the ability of comment on temporal evolution. The dynamic time point sampling in the present study highlights the earlier peak in this compound than the quantified 72 h time moment quantified by,[9] demonstrating the importance of tracking volatile evolution.

To further explore the fate of these middle-peaking compounds, Fig. 4 highlights downstream products that are generated by the continued metabolism of *Lp. plantarum*. Specifically, hexanoic acid (fatty, cheesy aroma) and ethyl hexanoate (fruit, pineapple aroma), which peak at 5 and 72 h, respectively, are both downstream reaction products of hexanal and 1-hexanol[9,53,54] reported the absence of hexanoic acid when *Lp. plantarum* was added in co-culture with *S. cerevisiae* compared with *S. cerevisiae* in mono-culture by 72 h of oat SSF. This is likely due to the earlier peak highlighted in the present study, and validates the further evolution to downstream products by the LAB. Specifically, *Lp plantarum* aldehyde and acetaldehyde dehydrogenases can oxidise aldehydes to yield carboxylic acids.[37,38] Moreover, the Erlich pathway can further enrich acids *via* α-keto acid intermediates in the degradation of proteins.[37] Specifically, 2-methyl-butanoic acid (cheesy aroma) also increased in *Lp. plantarum* SSF oats (not shown), which was likely produced from 2-methyl-butanal (apple, brandy aroma) *via* leucine dehydrogenase (Table S3). Acids can be further esterified with alcohols to yield esters such as ethyl-hexanoate (pineapple, floral aroma).[19] This explains the late peak in this compound as acids need to first be produced before they can be significantly enriched.

Ketones, such as 2-hydroxy-3-pentanone (earthy, nutty aroma), 2-nonanone (herbaceous aroma), and 3-heptanone (green, fruity aroma) increased throughout fermentation with *Lp. plantarum via* ketogenesis.[55] The former peaked after only 5 h of SSF, while the latter two after 48 h of fermentation. It is well known that LAB are good at producing ketones owing to their high level of Baeyer–Villiger monooxygenases.[56] These enzymes are involved in the β-oxidation and formation of β-ketoacids from hydrolysed lipids. This highlights the need to perform SSF for at least 48 h to enrich these compounds to a maximum if desired. The slight dip in 2-heptanone is in line with's[21] findings in a SmF system and can be attributed to *Lp. planatrum* reductases further reducing this to secondary

alcohols[9,57] reported no difference in 2-heptanone but an increase in 2-nonanone and 2-hydroxy-3-pentanone when *Lp. plantarum* was added in co-culture with *S. cerevisiae* compared to *S. cerevisiae* in mono-culture after 72 h of oat SSF. The present study, therefore, demonstrates the ability of *Lp. plantarum* to generate 2-heptanone in mono-culture, implying that *S. cerevisiae* is not solely responsible for its production, while this LAB is largely responsible for 2-nonanone and 2-hydroxy-3-pentanone production.[9] Volatile phenols such as 4-methoxy-vinyl phenol (clove-like aroma), mequinol (sweet, vanilla aroma) and 2-ethyl-phenol (mild, smokey aroma), all peaked near the midpoints of SSF with *Lp. plantarum* (Fig. 4).[58] The study by[9] also reported the increased 2-methoxy-4-vinylphenol levels when *Lp. plantarum* was added in co-culture with *S. cerevisiae* compared with *S. cerevisiae* in mono-culture after 72 h of oat SSF, while no detection of mequinol was reported for either system. The dynamic sampling in the present study, highlighting both compounds' peaks at 5–12 h, implies that[9] missed the peak in both compounds by 72 h, and *Lp. planatrum* is largely responsible for their production, as opposed to *S. cerevisiae*. The increase in these compounds signifies the decarboxylation and reduction of hydroxycinnamic acids within the oat substrate.[9,59] This is significant as phenols can have bioactive properties, which is a major focus of many SSF studies. The increase in these volatile phenols suggests that *Lp. plantarum* can successfully liberate these compounds from the oat matrix and/or further metabolise these into new phenol products. [9] Also reported the increase in volatile phenols such as mequinol.

Conclusions

In the present study, SSF of oats using *Lp. plantarum* was successfully tracked through fermentation characterisation and the evolution of volatile compounds over 120 h. *Lp. plantarum* showed expected fermentation profiles for pH and viable cell count changes over time, exhibiting the most extreme values by 12 h with a pH of 4.88 and a log CFU per g count of 9.01. The HS-SPME-GC-MS method was validated and successfully tracked the evolution of 51 volatiles and their chemical classes over time. Key findings were that after 120 h, aldehydes decreased by 12.7%, while phenols, aromatic compounds, alcohols, ketones, and carboxylic acids increased by 738.9%, 53.6%, 71.3%, 135.8%, and 80.7% respectively. Certain compounds, such as volatile phenols, were found to be maximised at mid-length (12 h) fermentation times with a 2007.9% increase, while others, such as ketones, were found to continue increasing up until 120 h. Through the modelling of the volatile data with linear PLS-R and non-linear RF-R, it was found that the non-linear model performed better for predicting SSF time (RMSE cv decreased 14.7%, R^2 cv increased 4.8%), accounting for the non-linear nature of *Lp. plantarum* volatile production. Further non-linear modelling may improve predictions further, although both models were able to separate samples over the SSF time. Feature selection of RF-R reinforced this argument by feature selecting a greater range of compounds, including more that peaked in the middle (12–48 h) of SSF. Overall, the characterisation of the SSF of oats with *Lp. plantarum* over time yielded

new information on the evolution of specific compounds, allowing for further manipulation of the SSF system to desired ends. Future work should focus on targeted analyses of feature-selected compounds in the present study, identifying and quantifying with standards over time, to maximise desired outcomes, such as enriched phenolic profiles, or specific flavour-active compounds. Such work should also be extended to non-volatile fractions, informed by the metabolic inferences made in the present study.

Author contributions

Conflicts of interest

There are no conflicts to declare.

Data availability

The data supporting this article (such as the raw abundance or peak areas) have been included as part of the SI. See DOI: https://doi.org/10.1039/d5fb00213c.

Acknowledgements

References

1 S. M. Gomes, A. M. Carvalho, A. S. Cantalice, A. R. Magalhães, D. Tregidgo, D. V. B. de Oliveira, E. B. da Silva, E. J. de Menezes-Neto, J. K. da Silva Maia and R. A. F. de Gusmão, *Environ. Sci. Pol.*, 2024, **161**, 103885.

2 S. S. Myers, M. R. Smith, S. Guth, C. D. Golden, B. Vaitla, N. D. Mueller, A. D. Dangour and P. Huybers, *Annu. Rev. Publ. Health*, 2017, **38**, 259–277.

3 Plant and Food Research Ltd & Ministry of Health., New Zealand Food Composition Database, 2024, https://www.foodcomposition.co.nz/, accessed 6/03/2024.

4 V. Sterna, S. Zute and L. Brunava, *Agric. Agric. Sci. Procedia.*, 2016, **8**, 252–256.

5 S. Green, G. T. Eyres, D. Agyei and B. Kebede, *Compr. Rev. Food Sci. Food Saf.*, 2024, **23**, e70070.

6 A. Pandey, *Biochem. Eng. J.*, 2003, **13**, 81–84.

7 H. Wu, H.-N. Liu, A.-M. Ma, J.-Z. Zhou and X.-D. Xia, *LWT*, 2022, **154**, 112687.

8 R. Tosun and S. Yasar, *J. Food Meas. Char.*, 2023, **17**, 984–997.

9 J. Sun, A.-A. Waleed, M. Fan, Y. Li, H. Qian, L. Fan and L. Wang, *Food Chem.*, 2023, 137813.

10 L. A. F. Castaneda, S. Saini, O. Laaksonen, A. Kårlund, S.-l. L. Leong, W. R. Newson, V. Passoth, K. Hanhineva, M. Langton and G. Zamaratskaia, *Curr. Res. Food Sci.*, 2025, 101029.

11 X. M. Feng, T. O. Larsen and J. Schnürer, *Int. J. Food Microbiol.*, 2007, **113**, 133–141.

12 W. Wei, Y. Shen, W. Cheng and W. Zhang, *LWT*, 2023, **188**, 115465.

13 N. Garcia-Gonzalez, N. Battista, R. Prete and A. Corsetti, *Microorganisms*, 2021, **9**, 349.

14 I. Salmeron, P. Fuciños, D. Charalampopoulos and S. S. Pandiella, *Food Chem.*, 2009, **117**, 265–271.

15 E. Di Stefano, N. Hüttmann, P. Dekker, M. M. Tomassen, T. Oliviero, V. Fogliano and C. C. Udenigwe, *Food Funct.*, 2024, **15**, 11220–11235.

16 J. M. Lorenzo, P. E. Munekata, R. Dominguez, M. Pateiro, J. A. Saraiva and D. Franco, in *Innovative Technologies for Food Preservation*, Elsevier, 2018, pp. 53–107.

17 L. Pompa, A. Montanari, A. Tomassini, M. M. Bianchi, W. Aureli, A. Miccheli, D. Uccelletti and E. Schifano, *Microorganisms*, 2023, **11**, 1087.

18 P. Russo, M. L. V. de Chiara, V. Capozzi, M. P. Arena, M. L. Amodio, A. Rascón, M. T. Dueñas, P. López and G. Spano, *LWT – Food Sci. Technol.*, 2016, **68**, 288–294.

19 Z. He, H. Zhang, T. Wang, R. Wang and X. Luo, *Foods*, 2022, **11**, 3230.

20 M. Wronkowska, D. Rostek, M. Lenkiewicz, E. Kurantowicz, T. G. Yaneva and M. Starowicz, *J. Cereal. Sci.*, 2022, **103**, 103392.

21 S. M. Lee, J. Oh, B. S. Hurh, G. H. Jeong, Y. K. Shin and Y. S. Kim, *J. Food Sci.*, 2016, **81**, C2915–C2922.

22 W. C. Vong, X. Y. Hua and S.-Q. Liu, *LWT*, 2018, **90**, 316–322.

23 N. Horlacher, J. King, S. Y. Leong, D. Agyei, G.-J. Moggré, K. Sutton and I. Oey, *LWT*, 2025, **220**, 117587.

24 X. Li, I. Oey and B. Kebede, *Food Res. Int.*, 2022, **157**, 111243.

25 R. High, P. Bremer, B. Kebede and G. T. Eyres, *Molecules*, 2019, **24**, 1917.

26 B. Kebede, V. Ting, G. Eyres and I. Oey, *Foods*, 2020, **9**, 165.

27 L. G. Johnsen, P. B. Skou, B. Khakimov and R. Bro, *J. Chromatogr., A*, 2017, **1503**, 57–64.

28 A. Warburton, P. Silcock and G. T. Eyres, *Food Res. Int.*, 2022, **161**, 111885.

29 R. D. C. Team, (No Title), 2010.

30 R. Team, (No Title), 2015.

31 M. H. Zwietering, I. Jongenburger, F. M. Rombouts and K. Van't Riet, *Appl. Environ. Microbiol.*, 1990, **56**, 1875–1881.

32 H. M. Patel, R. Wang, O. Chandrashekar, S. S. Pandiella and C. Webb, *Biotechnol. Prog.*, 2004, **20**, 110–116.

33 K. Papadimitriou, Á. Alegría, P. A. Bron, M. De Angelis, M. Gobbetti, M. Kleerebezem, J. A. Lemos, D. M. Linares, P. Ross and C. Stanton, *Microbiol. Mol. Biol. Rev.*, 2016, **80**, 837–890.

34 L. Chen, Z. Zhao, W. Yu, L. Zheng, L. Li, W. Gu, H. Xu, B. Wei and X. Yan, *AMB Express*, 2021, **11**, 1–11.

35 Q. Ma, N. Hamid, A. Bekhit, J. Robertson and T. Law, *Microchem. J.*, 2013, **111**, 16–24.

36 R. D. Astuti, D. L. N. Fibri, D. D. Handoko, W. David, S. Budijanto and H. Shirakawa, *Fermentation*, 2022, **8**, 120.

37 S. Try, A. Voilley, T. Chunhieng, J. De-Coninck and Y. Waché, *Appl. Microbiol. Biotechnol.*, 2018, **102**, 7239–7255.

38 B. A. Smit, W. J. Engels and G. Smit, *Appl. Microbiol. Biotechnol.*, 2009, **81**, 987–999.

39 W. Zhang, F. Zhao, F. Zhao, T. Yang and S. Liu, *Sci. Rep.*, 2019, **9**, 2538.

40 M. Spaggiari, A. Ricci, L. Calani, L. Bresciani, E. Neviani, C. Dall'Asta, C. Lazzi and G. Galaverna, *LWT*, 2020, **118**, 108668.

41 A. B. Medeiros, A. Pandey, R. J. Freitas, P. Christen and C. R. Soccol, *Biochem. Eng. J.*, 2000, **6**, 33–39.

42 A. Khorsandi, The use of solid-state fermentation to improve the protein quality, functionality and flavour of pulse protein isolates, PhD thesis, University of Saskatchewan, 2022.

43 R. J. McGorrin, *J. Agric. Food Chem.*, 2019, **67**, 13778–13789.

44 J. Sim, C. Mcgoverin, I. Oey, R. Frew and B. Kebede, *J. Sci. Food Agric.*, 2023, **103**, 4704–4718.

45 M. Aria, C. Cuccurullo and A. Gnasso, *Mach. Learn. Appl.*, 2021, **6**, 100094.

46 S. Guo, T. Wu, C. Peng, J. Wang, T. Sun and H. Zhang, *J. Dairy Sci.*, 2021, **104**, 8541–8553.

47 R. High, G. T. Eyres, P. Bremer and B. Kebede, *Food Chem.*, 2021, **347**, 128955.

48 C. F. Dormann, J. Elith, S. Bacher, C. Buchmann, G. Carl, G. Carré, J. R. G. Marquéz, B. Gruber, B. Lafourcade and P. J. Leitão, *Ecography*, 2013, **36**, 27–46.

49 E. J. Want, I. D. Wilson, H. Gika, G. Theodoridis, R. S. Plumb, J. Shockcor, E. Holmes and J. K. Nicholson, *Nat. Protoc.*, 2010, **5**, 1005–1018.

50 J. Kun, Y. Yang, J. Sun, H. Dai, Z. Luo and H. Tong, *LWT*, 2025, **215**, 117177.

51 L. Yuan, M. Li, X. Xu, X. Shi, G. Chen, F. Lao and J. Wu, *Front. Food*, 2024, **5**, 508–521.

52 Z. Wang, J.-J. He, X.-X. Liu, H.-L. Shi, Y.-F. Lu, J.-Y. Shi, Y.-C. Kan, L.-G. Yao and C.-D. Tang, *Electron. J. Biotechnol.*, 2023, **63**, 1–9.

53 R. Ríos-Reina, R. Aparicio-Ruiz, M. T. Morales and D. L. García-González, *Food Chem.*, 2023, **399**, 133942.

54 Y. Xiao, H. Chen, Y. Chen, C.-T. Ho, Y. Wang, T. Cai, S. Li, J. Ma, T. Guo and L. Zhang, *Food Res. Int.*, 2024, **197**, 115219.

55 R. Attaie, *J. Dairy Sci.*, 2009, **92**, 2435–2443.

56 A. Beier, V. Hahn, U. T. Bornscheuer and F. Schauer, *AMB Express*, 2014, **4**, 1–8.

57 W. C. Vong and S. Q. Liu, *J. Sci. Food Agric.*, 2017, **97**, 135–143.

58 D. Langos and M. Granvogl, *J. Agric. Food Chem.*, 2016, **64**, 2325–2332.

59 I. Bautista-Hernández, R. Gómez-García, C. N. Aguilar, G. C. Martínez-Ávila, C. Torres-León and M. L. Chávez-González, *Agriculture*, 2024, **14**, 1342.